

Optimal Design Solutions for Permanent Magnet Synchronous Machines

Tiberiu TUDORACHE¹, Mihail POPESCU²

¹University Politehnica of Bucharest, 060042, Romania

²Research Institute for Electrical Machines (ICPE-ME), 050881, Bucharest, Romania
tudorach@amotion.pub.ro

Abstract—This paper presents optimal design solutions for reducing the cogging torque of permanent magnets synchronous machines. A first solution proposed in the paper consists in using closed stator slots that determines a nearly isotropic magnetic structure of the stator core, reducing the mutual attraction between permanent magnets and the slotted armature. To avoid complications in the windings manufacture technology the stator slots are closed using wedges made of soft magnetic composite materials. The second solution consists in properly choosing the combination of pole number and stator slots number that typically leads to a winding with fractional number of slots/pole/phase. The proposed measures for cogging torque reduction are analyzed by means of 2D/3D finite element models developed using the professional Flux software package. Numerical results are discussed and compared with experimental ones obtained by testing a PMSM prototype.

Index Terms—optimal design, permanent magnet machines, numerical analysis, experimental validation.

I. INTRODUCTION

One of the electrical machines increasingly used in industry is the Permanent Magnet Synchronous Machine (PMSM). Its advantages compared to the electromagnetic excitation machines consist in a superior efficiency, lack of sliding contacts and high energy density per volume unit [1], [2].

The PMSM based applications are very numerous in the range of small power. The gradual price decrease of high energy rare earth permanent magnets of NdFeB type, encouraged the use of PMSM in medium and high power applications such as wind turbines, propulsion systems, industrial robots, machine tools, etc. [3]–[6].

A specific application where PMSM is more and more preferred is the low speed and high torque electric drive systems. This type of drives does not include gearbox, the electric machine being directly driven by the motion control system. The removal of the gearbox that typically represents a source of important losses and involves high maintenance costs is very attractive and permits the simplification of the drive cinematic conversion chain.

The electric machine in case of high torque applications should operate at low rotational speeds and thus it should have a large number of magnetic poles.

A typical drawback of multi-pole PMSM is represented by the existence of the cogging torque that appears due to the mutual attraction between rotor and stator magnetic

armatures of the machine. This phenomenon appears due to the non-isotropic magnetic structure of the stator armature as consequence of the presence of open or semi-open stator slots where the windings are placed. The interaction between the permanent magnets and the slotted armature generates preferential directions of minimum magnetic energy that the rotor armature tends to align to.

The cogging torque superposes over the electromagnetic torque and generates vibrations and stress at the machine bearings level.

Correctly designed PMSMs are generally characterized by cogging torque values smaller than 1.5 - 2.5% of the rated torque [7]. In order to comply with these constraints, the design of PMSM should be based on reliable 2D/3D finite element models able to precisely evaluate the cogging torque values.

Various methods to reduce the cogging torque of PMSM are proposed. They consist in using non-uniform airgap structures [8]–[10], axial magnets pairing [11], stator skewing [12], slot opening shift [13] etc. Syntheses of several cogging torque reduction methods are also presented in [14], [15].

Two methods for minimizing PMSM cogging torque values will be investigated and compared in this paper. The physical support for this study is represented by several variants of a PMSM characterized by the main data: rated power 400 VA, 36 stator straight slots, rated speed 1600 rpm, lamination stack length 15 mm, airgap thickness 0.5 mm. The permanent magnets are half-buried in the rotor core and are radially magnetized.

II. FINITE ELEMENT 2D MODEL OF PMSG. COGGING TORQUE COMPUTATION

The evaluation of PMSM cogging torque is based on a 2D parallel-type Finite Element (FE) model of the machine. The computation domain is represented by a cross section through the machine, Fig. 1. This first analysis is carried out on a reference configuration of PMSM characterized by 12 magnets (19 mm width, 6.5 mm height and 44 mm curvature radius), symmetrically placed at the outer rotor surface. The governing differential equation of the magneto-static field is:

$$\nabla \times \left[\left(\frac{1}{\mu} \nabla \times \mathbf{A} \right) \right] = \nabla \times \left[\left(\frac{1}{\mu} \right) \mathbf{B}_r \right] \quad (1)$$

where \mathbf{A} stands for the magnetic vector potential, μ for magnetic permeability of magnetic cores, \mathbf{B}_r for remnant

The work has been co-funded by the Sectoral Operational Programme Human Resources Development 2007-2013 of the Romanian Ministry of Labour, Family and Social Protection through the Financial Agreement POSDRU/89/1.5/S/62557.

magnetization of permanent magnets.

The finite element discretization of the computation domain consists of around 21800 second order elements of triangle shape (~ 82000 nodes) with smaller size in the airgap region where the most part of the magnetic energy is located, Fig. 2.

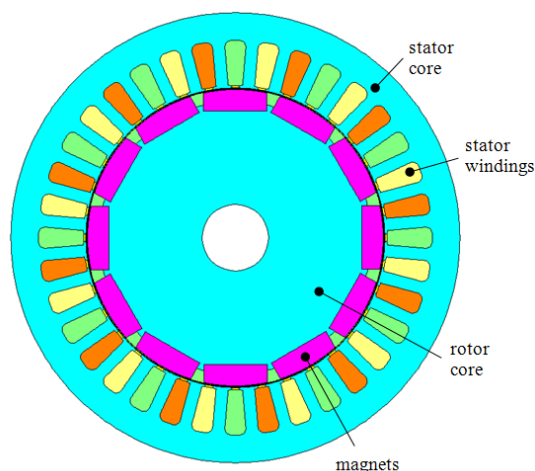


Figure 1. FE computation domain of 2D magnetostatic field problem for a PMSM with 36/12 slot/pole combination.

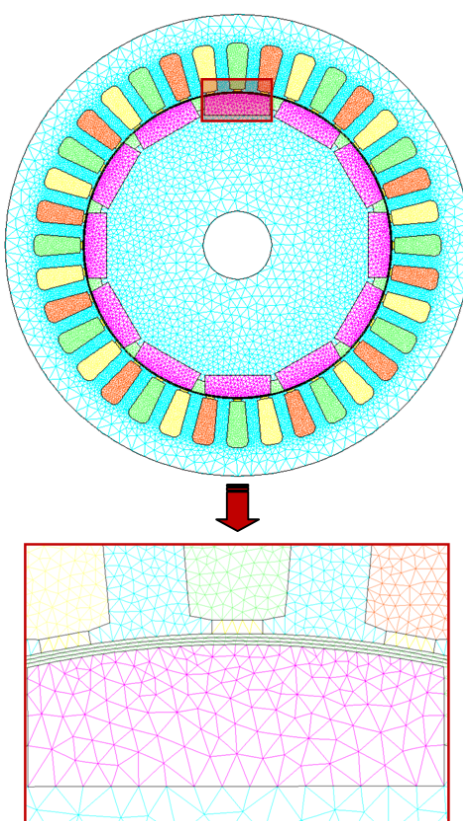


Figure 2. FE discretization of 2D computation domain.

In order to obtain good accuracy cogging torque numerical results we used three layers of finite elements in the airgap region. By using a single or two layers of finite elements in that region non-negligible numerical errors may appear in the computation of cogging torque values.

The stator magnetic core is made of laminations of M600-50A type characterized by the B-H curve presented in Fig. 3, and the rotor magnetic core is made of OL 37 steel. The permanent magnets are made of NdFeB of N35 type

with remnant magnetic flux density $B_r = 1.23$ T and $\mu_r = 1.088$.

By solving the 2D magneto-static field problem using the Flux software package we obtained the magnetic flux density and field lines spectrum shown in Fig. 4.

By solving the 2D magneto-static field problem for successive relative stator/rotor positions of the PMSM, we obtained the cogging torque oscillations computed with the Virtual Works Method, Fig. 5.

Studying the numerical results in Fig. 5 we can notice unacceptably high values of the cogging torque that can affect the effective operation of the PMSM. The cogging torque peak value in this case is around 1.87 Nm, which means more than 50 % of the rated torque.

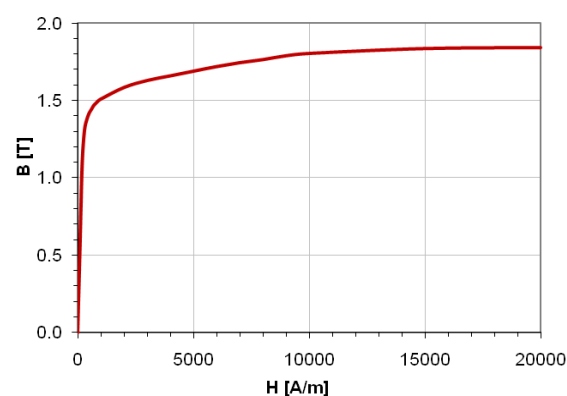


Figure 3. B-H curve for M600-50 A laminations.

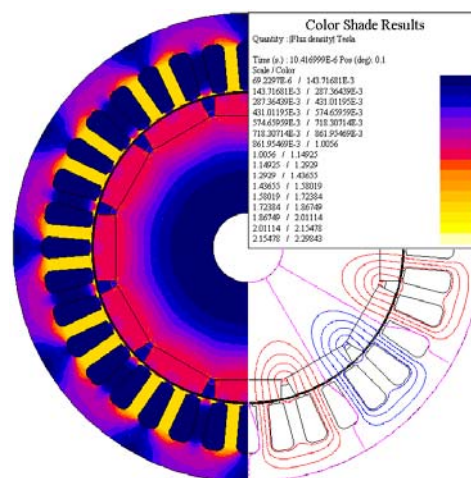


Figure 4. Magnetic flux density and field lines.

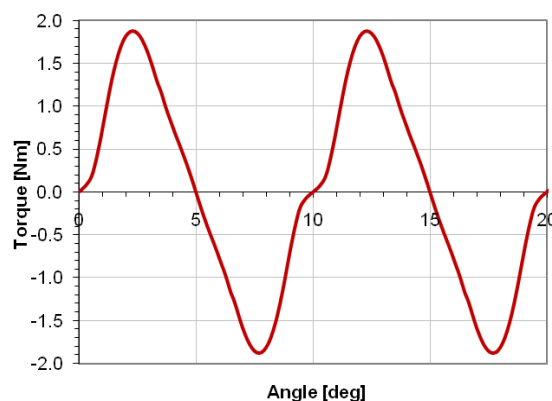


Figure 5. Cogging torque versus rotor position for a PMSM with 36/12 slot/pole combination.

III. 3D NUMERICAL MODELING OF 36/12 PMSM. COGGING TORQUE COMPUTATION

Since the analyzed PMSM has a large number of poles, large diameter and small length, the frontal effects could be non-negligible. A consideration of these effects requires a complex 3D numerical analysis of the machine. The numerical model used for 3D computations is based on magnetic scalar potential ϕ formulation characterized by the following partial differential equation:

$$\text{div}[-\mu(\mathbf{H})\text{grad}\phi + \mathbf{B}_r] = 0 \quad (2)$$

where μ represents the magnetic permeability, \mathbf{H} the magnetic field strength and \mathbf{B}_r the remnant magnetic flux density.

The computation domain that takes into account the axial physical symmetry of the PMSM is reduced to only half of the machine in axial direction, Fig. 6. The finite element discretization of the computation domain has 879539 second order elements their size being refined in the airgap region. In order to compute with precision the cogging torque values, Fig. 7, three layers of finite element were used in the airgap region.

On the symmetry plane of the computation domain tangential field condition was imposed ($\mathbf{B} \cdot \mathbf{n} = 0$). In order to model the exterior boundary (open boundary problem), the "infinite box" structure implemented in Flux3D was used. This structure transforms the exterior infinite space into a limited space by means of a Kelvin type transformation.

By successive 3D numerical simulations we computed the cogging torque values for different relative rotor/stator positions, the numerical results being presented in Fig. 8 in comparison with the 2D results.

Important hardware resources were needed for the 3D numerical analysis. The average computation time for a single rotor/stator relative position was larger than 9000 seconds on a PC equipped with Intel Xeon Quad Core E5420 processor and 16 GB of RAM. By comparison, a similar 2D computation required only about 4.5 seconds, being about 2000 times faster than a 3D computation.

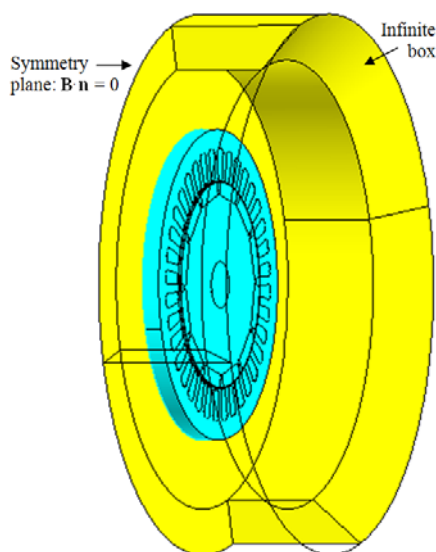


Figure 6. Computation domain for 3D FE analysis.

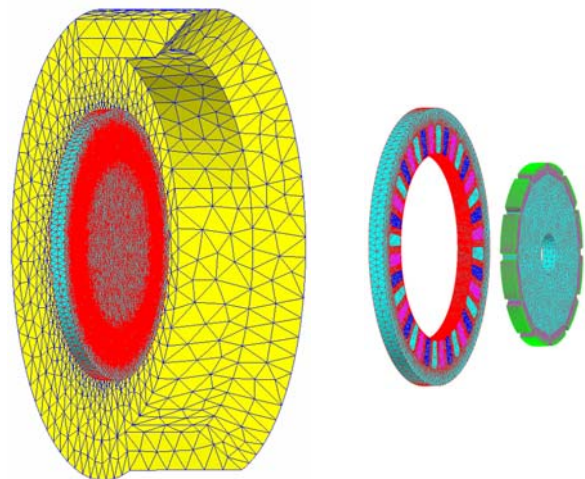


Figure 7. FE discretization of 3D computation domain (exploded view)

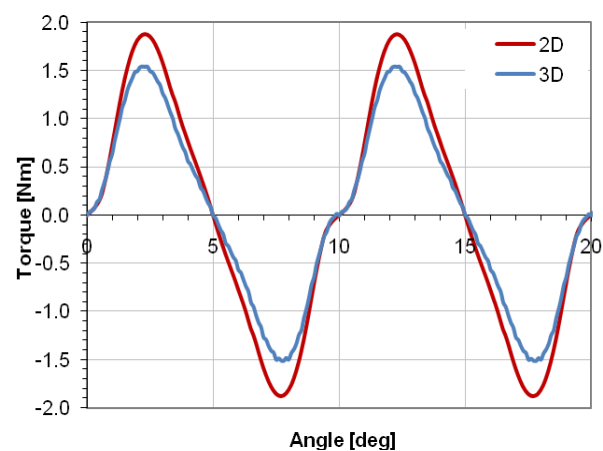


Figure 8. Cogging torque versus rotor position (2D and 3D results) for a PMSM with 36/12 slot/pole combination.

The profiles of the 3D and 2D results of the cogging torque are comparable but with some relative differences. The smaller values of the cogging torque in the 3D analysis in comparison with the 2D approach are not very surprising. In the 3D analysis the magnetic flux density values decline naturally at the frontal ends of the PMSM (as in reality), decreasing thus the torque/volume density of the machine. In the 2D approach, the magnetic flux density is constant in the axial direction of the machine, leading to higher cogging torque values. Another cause of the discrepancy between 2D and 3D numerical results could be the different nature of magnetic field formulations used in the two approaches.

The huge computation effort required for a 3D analysis determined us to continue the investigations of the PMSM using the 2D approach. A 3D analysis remains however a useful option for validating 2D simulation results before building the prototype.

IV. CLOSED STATOR SLOTS

A good solution for reducing the cogging torque of PMSM consists in adopting a geometrical configuration of the machine with closed stator slots. By using this arrangement the machine will have a nearly isotropic electromagnetic structure of the stator that entails a remarkable reduction of cogging torque peak values.

The closed stator slots solution supposes a more complicated manufacturing process of stator windings that could be an important drawback for the mass production of the PMSM. A simple method to overcome this shortcoming is to close the stator slots with wedges made of Soft Magnetic Composite (SMC) materials (Somaloy class). The effect of this solution in terms of cogging torque is similar to the case of using stator lamination stack with closed slots, but it has the merit of keeping unchanged the manufacturing technology of the lamination stack and stator winding as in the case of classical semi-open slots machines.

The computation results for the PMSM with stator slots closed with SMC wedges made of Somaloy 500 [16], prove a reduction of cogging torque peak values of roughly 3.15 times, from 1.87 Nm to 0.593 Nm, Fig. 9.

V. PROPER CHOICE OF SLOTS/POLES NUMBER COMBINATION

Another method for cogging torque reduction of PMSM consists in a proper choice of the slot/pole number combination. The optimum choice for a minimum cogging torque should be done so as the greatest common divisor t of Z (number of stator slots) and $2p$ (number of rotor poles) to be minimum:

$$t = \gcd(Z, 2p), \text{ should be minimum,} \quad (3)$$

The number t is an integer that represents the number of magnets that are attracted at a given time instant by the Z stator teeth. A minimum t number could be for example a value equal with 2.

The relation linking the number of slots Z , the number of slots/pole/phase q and the number of poles $2p$ is $Z = 2mpq$.

In order to obtain a symmetrical and balanced winding we should respect the relation $Z/m = \text{integer}$. If we consider a three phase PMSM ($m = 3$) with $Z = 36$ stator slots we get $2pq = 12$.

In order to obtain $t = 2$, we must have the number of poles $2p \in \{2, 10, 14, 22 \dots\}$ and the corresponding $q \in \{6, 6/5, 6/7, 6/11 \dots\}$.

The variation with the number of poles of the winding factor k_w , number t and number of slots/pole/phase q is presented in Fig. 10. If we study these curves we can identify the suitable numbers of poles that correspond to the smallest number t . We will choose $2p = 10$, that means a 36/10 slot/pole combination PMSM, with fractional $q = 6/5$.

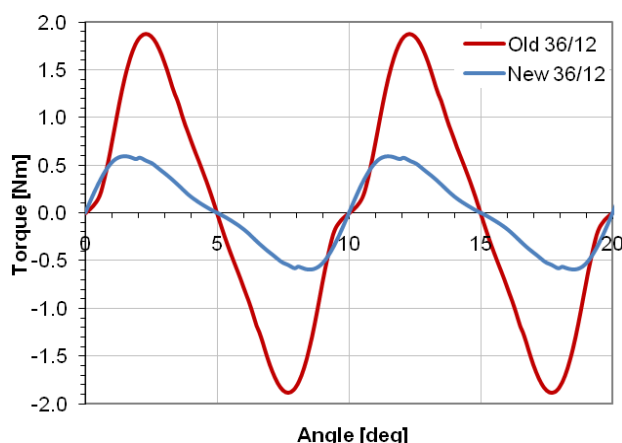


Figure 9. Cogging torque oscillations for PMSM with closed stator slots.

After having adapted the 2D model of the machine for 36/10 combination we successively solved the associated magneto-static field problem for different rotor/stator relative positions and we obtained the cogging torque oscillations. The numerical results presented in Fig. 11 prove that the cogging torque peak values in this case are much smaller than for 36/12 combination (about 69.26 times from 1.87 Nm to only 0.027 Nm).

Comparing the numerical results in Figs. 9 and 11 we can notice that the last cogging torque reduction solution is more suitable than the first one. This last solution leads to a cogging torque peak value of about 1.13% of the rated electromagnetic torque of the machine complying with quality norms imposed nowadays.

The stator three-phase winding of the PMSM in case of the 36/12 slot/pole combination is classical ($q = 1$ and coil opening $y = 3$), while the winding for the 36/10 slot/pole combination is more complex, with unequal coils per phase, Fig. 12.

The phase-to-phase e.m.f. obtained for the machine rated speed (1600 rpm) shows a quasi-sinusoidal wave-form with reduced harmonics content, this feature representing an advantage in many PMSM applications, Figs. 13 and 14.

Successive simulations for different load levels (resistive and inductive loads) and rated speed allowed us to evaluate the voltage characteristic (terminal voltage versus load current) of the 36/10 PMSM and its power curve (apparent power versus load current), Figs. 15 and 16.

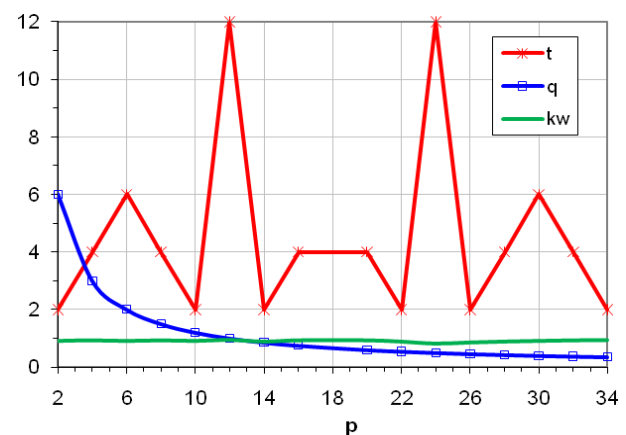


Figure 10. Variation of quantities k_w , t and q with the number of poles in case of $Z = 36$ slots.

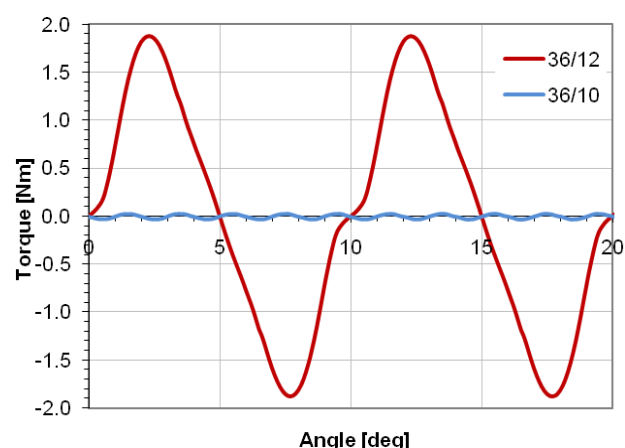


Figure 11. Cogging torque oscillations for 36/12 and 36/10 PMSMs.

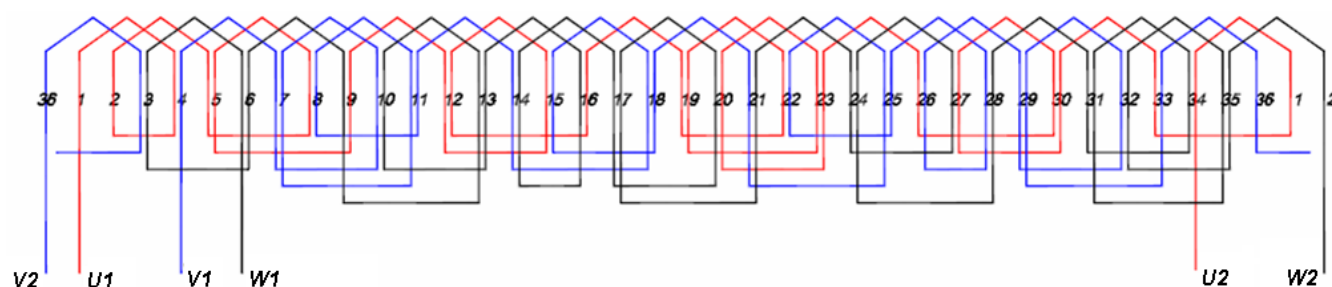


Figure 12. Winding diagram for the 36/10 slot/pole.

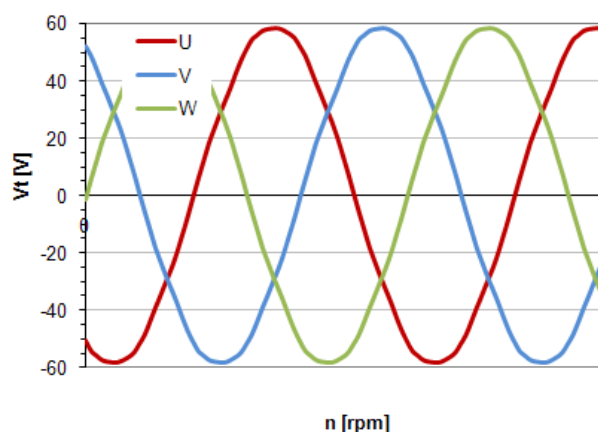


Figure 13. E.m.f. for 36/10 PMSM under no-load.

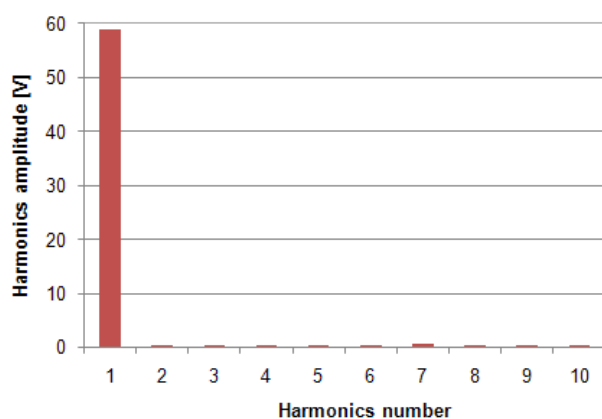


Figure 14. E.m.f. spectrum analysis of 36/10 PMSM.

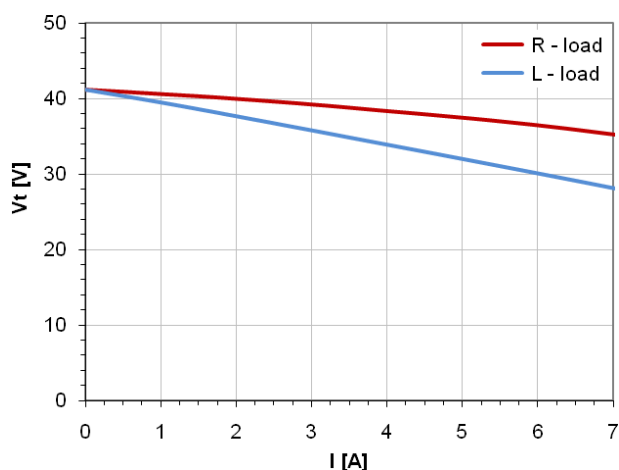


Figure 15. Voltage characteristic of 36/10 PMSM for R and L load.

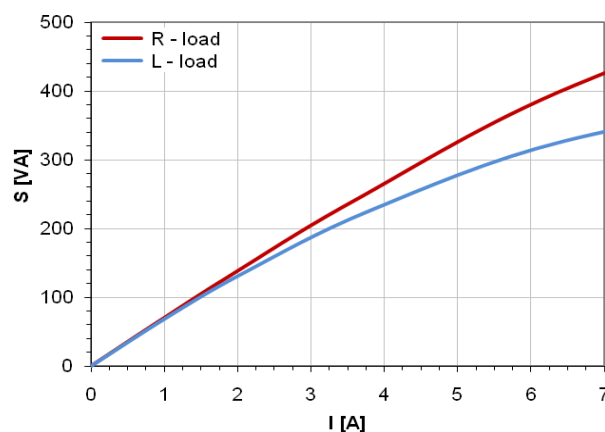


Figure 16. Power curve of 36/10 PMSM in case of R and L load.

The decrease of terminals voltage from no-load to rated load is of about 5.22 V (12.66%) for resistive load and 11.92 V (28.92%) for inductive load, Fig. 15. The maximum output apparent power produced by the PMSM is of about 560 VA in case of resistive load and 384 VA in case of inductive load.

VI. EXPERIMENTAL VALIDATION OF NUMERICAL RESULTS

The validation of numerical simulation results was carried out on a 36/10 pole/slot PMSM prototype manufactured by ICPE-ME. Figs. 17 - 18. The experimental facility employed for measurements uses an inverter fed induction motor equipped with vector control to rotate the tested PMSM prototype at different speeds.

A good agreement can be noticed between numerical and simulation results of the e.m.f. (phase-to-phase voltage) of the PMSM versus machine speed, Fig. 19.

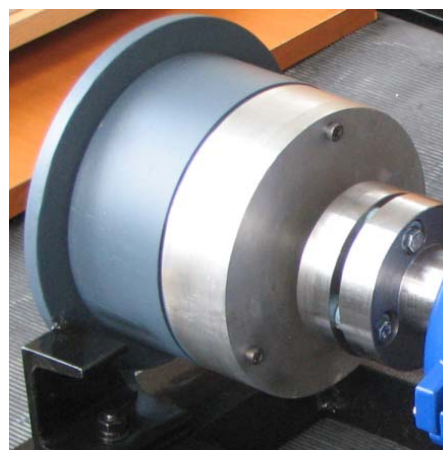


Figure 17. PMSM prototype with 36/10 slot/pole combination, manufactured by ICPE-ME.

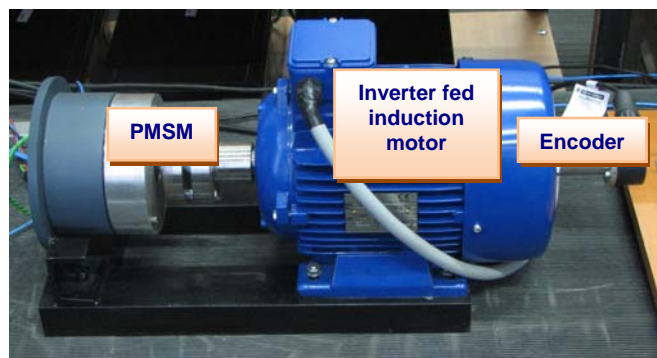


Figure 18. Experimental setup used for validation of numerical results of the 36/10 PMSM.

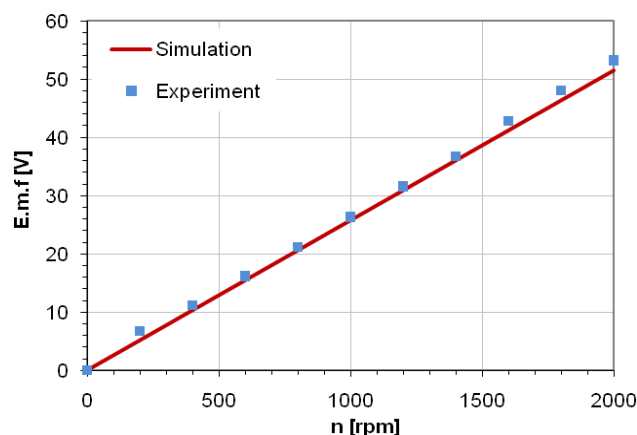


Figure 19. E.m.f. versus speed for 36/10 PMSM under no-load.

VII. CONCLUSION

The research results presented in the paper proves the usefulness of finite element numerical models for the optimal design of PMSM. The differences between the cogging torque numerical results obtained by 2D and 3D analyses are relatively reduced. Thus we may consider that the 2D analysis, much more economical from computation effort point of view, offers information accurate enough to be used for the numerical analysis of PMSM.

Two methods used to reduce the cogging torque values, were analyzed in the paper. The first one consists in closing the stator slots with SMC made wedges and the second one consists in optimally choosing the slot-pole combination. The second methods proved to be more efficient leading to a drastic reduction of cogging torque peak values from 1.87 Nm to only 0.027 Nm.

A combination between the two cogging torque reduction methods is expected to produce still better results.

The first cogging torque reduction method is technologically more complicated requiring the construction of special wedges made of SMC, while the second method requires only a slightly more complex stator winding diagram.

Numerical results were validated by experimental measurements carried out on a PMSM prototype manufactured by ICPE-ME.

Equipped with adequate electronics the developed 36/10 PMSM could be used as generator for small power 48/24/12 V battery-charging wind systems.

REFERENCES

- [1] I. A. Viorel, L. Strete, K. Hameyer, "Construction and Design of a Modular Permanent Magnet Transverse Flux Generator", *Advances in Electrical and Computer Engineering Journal*, Vol. 10, No. 1, pp. 3-6, 2010. [Online]. Available: <http://dx.doi.org/10.4316/aece.2010.01001>
- [2] S. Hosseini, J. S. Moghani, B. B. Jensen, "Accurate Modeling of a Transverse Flux Permanent Magnet Generator Using 3D Finite Element Analysis", *Advances in Electrical and Computer Engineering Journal*, Vol. 11, No. 3, pp. 115-120, 2011. [Online]. Available: <http://dx.doi.org/10.4316/aece.2011.03019>
- [3] B. Abdi, J. Milimonfared, J. Shokrollahi Moghani, A. Kashefi Kaviani, "Simplified Design and Optimization of Slotless Synchronous PM Machine for Micro-Satellite Electro-Mechanical Batteries", *Advances in Electrical and Computer Engineering Journal*, Vol. 9, No. 3, pp. 84-88, 2009. [Online]. Available: <http://dx.doi.org/10.4316/aece.2009.03015>
- [4] P. Zheng, J. Zhao, R. Liu, C. Tong, Q. Wu, "Magnetic Characteristics Investigation of an Axial-Axial Flux Compound-Structure PMSM Used for HEVs", *IEEE Trans. Magn.*, Vol. 46, No. 6, pp. 2191 - 2194, 2010. [Online]. Available: <http://dx.doi.org/10.1109/TMAG.2010.2042042>
- [5] J. Sopanen, V. Ruuskanen, J. Nerg and J. Pyrhonen, "Dynamic Torque Analysis of a Wind Turbine Drive Train Including a Direct-Driven Permanent Magnet Generator", *Trans. Ind. Electron.*, Vol. 58, No. 9, pp. 3859 - 3867, 2010. [Online]. Available: <http://dx.doi.org/10.1109/TIE.2010.2087301>
- [6] B. Vaseghi, N. Takorabet, F. Meibody-Tabar, "Investigation of a Novel Five-Phase Modular Permanent-Magnet In-Wheel Motor", *IEEE Trans. Magn.*, Vol. 47, No. 10, pp. 4084- 4087, 2011. [Online]. Available: <http://dx.doi.org/10.1109/TMAG.2011.2150207>
- [7] T. Tudorache, L. Melcescu, M. Popescu, M. Cistelean, "Finite Element Analysis of Cogging Torque in Low Speed Permanent Magnets Wind Generators", *Proc. of International Conference on Renewable Energies and Power Quality (ICREPQ 2008)*, Paper 412, 2008, Spain.
- [8] Y. Tomigashi, T. Ueta, K. Yokotani, K. Ikegami, "Reducing Cogging Torque of Interior Permanent Magnet Synchronous Motor for Electric Bicycles", *Proc. of the European Conference on Power Electronics and Applications (EPE 2005)*, P.8, 2005, Germany.
- [9] A. Jabbari, M. Shakeri, A. S. Gholamian, "Rotor Pole Shape Optimization of Permanent Magnet Brushless DC Motors Using the Reduced Basis Technique", *Advances in Electrical and Computer Engineering Journal*, Vol. 9, No. 2, pp. 75-81, 2009. [Online]. Available: <http://dx.doi.org/10.4316/aece.2009.02012>
- [10] A. Jabbari, M. Shakeri, A. Nabavi Niaki, "Iron Pole Shape Optimization of IPM Motors Using an Integrated Method", *Advances in Electrical and Computer Engineering Journal*, Vol. 10, No. 1, pp. 67-70, 2010. [Online]. Available: <http://dx.doi.org/10.4316/aece.2010.01012>
- [11] W. Fei and P. C. K. Luk, "A New Technique of Cogging Torque Suppression in Direct-Drive Permanent Magnet Brushless Machines", *International IEEE Electric Machines and Drives Conference (IEMDC 2009)*, pp. 9-16, 2009, USA. [Online]. Available: <http://dx.doi.org/10.1109/IEMDC.2009.5075176>
- [12] T. Tudorache, L. Melcescu, M. Popescu, "Methods for Cogging Torque Reduction of Directly Driven PM Wind Generators", *Proc. of IEEE Conference on Optimization of Electrical and Electronics Equipment (OPTIM 2010)*, 2010, Romania. [Online]. Available: <http://dx.doi.org/10.1109/OPTIM.2010.5510390>
- [13] S. A. Saied, K. Abbaszadeh, "Cogging Torque Reduction in Brushless DC Motors Using Slot-Opening Shift", *Advances in Electrical and Computer Engineering Journal*, Vol. 9, No. 1, pp. 28-33, 2009. [Online]. Available: <http://dx.doi.org/10.4316/aece.2009.01005>
- [14] M. S. Islam, S. Mir, T. Sebastian, "Issues in Reducing the Cogging Torque of Mass-Produced Permanent-Magnet Brushless DC Motor", *IEEE Trans. on Ind. Applications*, vol. 40, no. 3, May-June, 2004. [Online]. Available: <http://dx.doi.org/10.1109/TIA.2004.827469>
- [15] N. Bianchi, S. Bolognani, "Design Techniques for Reducing the Cogging Torque in Surface-Mounted PM Motors", *IEEE Trans. on Ind. Applications*, vol. 38, no. 5, Sept-Oct, 2002. [Online]. Available: <http://dx.doi.org/10.1109/TIA.2002.802989>
- [16] L. Hultman, O. Andersson, "Advances in SMC Technology – Materials and Applications", *Proc. of Advanced Magnetic Materials and their Applications*, 2009, Germany.